EUROPEAN ORGANIZATION FOR NUCLEAR RESEARCH (CERN)

Observation of two new Ξ_b^- baryon resonances

The LHCb collaboration[†]

Abstract

Two structures are observed close to the kinematic threshold in the $\Xi_b^0 \pi^-$ mass spectrum in a sample of proton-proton collision data, corresponding to an integrated luminosity of $3.0\,\mathrm{fb}^{-1}$, recorded by the LHCb experiment. In the quark model, two baryonic resonances with quark content bds are expected in this mass region: the spin-parity $J^P = \frac{1}{2}^+$ and $J^P = \frac{3}{2}^+$ states, denoted $\Xi_b^{\prime -}$ and Ξ_b^{*-}. Interpreting the structures as these resonances, we measure the mass differences and the width of the heavier state to be

$$
\begin{aligned}
m(\Xi_b^{\prime -}) - m(\Xi_b^0) - m(\pi^-) &= 3.653 \pm 0.018 \pm 0.006\,\mathrm{MeV}/c^2, \\
m(\Xi_b^{*-}) - m(\Xi_b^0) - m(\pi^-) &= 23.96 \pm 0.12 \pm 0.06\,\mathrm{MeV}/c^2, \\
\Gamma(\Xi_b^{*-}) &= 1.65 \pm 0.31 \pm 0.10\,\mathrm{MeV},
\end{aligned}
$$

where the first and second uncertainties are statistical and systematic, respectively. The width of the lighter state is consistent with zero, and we place an upper limit of $\Gamma(\Xi_b^{\prime -}) < 0.08\,\mathrm{MeV}$ at 95% confidence level. Relative production rates of these states are also reported.

[†]Authors are listed at the end of this Letter.

arXiv:1411.4849v1 [hep-ex] 18 Nov 2014

In the constituent quark model [1, 2], baryonic states form multiplets according to the symmetry of their flavor, spin, and spatial wavefunctions. The Ξ_b states form isodoublets composed of a Ξ_b^0 (bsu) and a Ξ_b^- (bsd) state. Three such Ξ_b isodoublets that are neither orbitally nor radially excited are expected to exist, and can be categorized by the spin j of the su or sd diquark and the spin-parity J^P of the baryon: one with $j = 0$ and $J^P = \frac{1}{2}^+$, one with $j = 1$ and $J^P = \frac{1}{2}^+$, and one with $j = 1$ and $J^P = \frac{3}{2}^+$. This follows the same pattern as the well-known Ξ_c states [3], and we therefore refer to these three isodoublets as the Ξ_b, the Ξ_b', and the Ξ_b^*. The spin-antisymmetric $J^P = \frac{1}{2}^+$ state, observed by multiple experiments [4–11], is the lightest and therefore decays through the weak interaction. The others should decay predominantly strongly through a P-wave pion transition ($\Xi_b^{(',*)} \to \Xi_b \pi$) if their masses are above the kinematic threshold for such a decay; otherwise they should decay electromagnetically ($\Xi_b^{(',*)} \to \Xi_b \gamma$). Observing such electromagnetic decays at hadron colliders is challenging due to large photon multiplicities and worse energy resolution for low energy photons compared to charged particles.

There are numerous predictions for the mass spectrum of these low-lying states [12–19]. The consensus is that the isospin-averaged value of the mass difference $m(\Xi_b^*) - m(\Xi_b)$ is above threshold for strong decay but that the isospin-averaged difference $m(\Xi_b') - m(\Xi_b)$ is near the kinematic threshold. However, it is expected that the mass difference $m(\Xi_b'^-) - m(\Xi_b^0)$ is larger than $m(\Xi_b'^0) - m(\Xi_b^-)$ due to the relatively large isospin splitting between the charged and neutral Ξ_b states. For the ground state, the measured isospin splitting of $m(\Xi_b^-) - m(\Xi_b^0) = 5.92 \pm 0.64\,\text{MeV}/c^2$ [20] is in good agreement with the predicted value of $6.24 \pm 0.21\,\text{MeV}/c^2$ [13]. While the equivalent isospin splitting for the Ξ_b' and Ξ_b^* states is likely to be smaller due to differences in the hyperfine mass corrections, the mass difference $m(\Xi_b'^-) - m(\Xi_b^0)$ could well be 5–10 MeV/c^2 larger than $m(\Xi_b'^0) - m(\Xi_b^-)$. It is therefore plausible that the decay $\Xi_b'^- \to \Xi_b^0 \pi^-$ is kinematically allowed, while $\Xi_b'^0 \to \Xi_b^- \pi^+$ is not. This is consistent with the recent CMS observation [21] of a single peak in the $\Xi_b^- \pi^+$ mass spectrum, interpreted as the Ξ_b^{*0} resonance. We note that $\Xi_b'^0 \to \Xi_b^0 \pi^0$ may also be allowed even if $\Xi_b'^0 \to \Xi_b^- \pi^+$ is not.

In this Letter we present the results of a study of the $\Xi_b^0 \pi^-$ mass spectrum using pp collision data recorded by the LHCb experiment, corresponding to an integrated luminosity of $3.0\,\text{fb}^{-1}$. One third of the data was collected at a center-of-mass energy of $7\,\text{TeV}$ and the remainder at $8\,\text{TeV}$. We observe two highly significant structures, which are interpreted as the $\Xi_b'^-$ and Ξ_b^{*-} baryons. The properties of these new states are reported. Charge-conjugate processes are implicitly included.

The LHCb detector [22] is a single-arm forward spectrometer covering the pseudorapidity range $2 < \eta < 5$, designed for the study of particles containing b or c quarks. The detector includes a high-precision tracking system, which provides a momentum measurement with precision of about 0.5% from $2-100$ GeV/c and impact parameter resolution of approximately $20\,\mu\text{m}$ for particles with large transverse momentum (p_T). Ring-imaging Cherenkov detectors [23] are used to distinguish charged hadrons. Photon, electron and hadron candidates are identified using a calorimeter system, which is followed by detectors to identify muons [24].

The trigger [25] consists of a hardware stage, based on information from the calorimeter

and muon systems, followed by a software stage. The software trigger requires a two-, three- or four-track secondary vertex which is significantly displaced from all primary pp vertices (PVs) and for which the scalar p_{T} sum of the charged particles is large. At least one particle should have $p_{\mathrm{T}} > 1.7\,\mathrm{GeV}/c$ and be inconsistent with coming from any of the PVs. A multivariate algorithm [26] is used to identify secondary vertices consistent with the decay of a b hadron.

In the simulation, pp collisions are generated using PYTHIA [27] with a specific LHCb configuration [28]. Decays of hadrons are described by EVTGEN [29], in which final-state radiation is generated using PHOTOS [30]. The interaction of the generated particles with the detector, and its response, are implemented using the GEANT4 toolkit [31] as described in Ref. [32].

Signal candidates are reconstructed in the final state $\Xi_b^0\pi_{\mathrm{s}}^-$, where $\Xi_b^0 \to \Xi_c^+\pi^-$ and $\Xi_c^+ \to pK^-\pi^+$. The first pion is denoted π_{s}^- to distinguish it from the others. At each stage of the decay chain, the particles are required to meet at a common vertex with good fit quality. In the case of the $\Xi_b^0\pi_{\mathrm{s}}^-$ candidate, this vertex is constrained to be consistent with one of the PVs in the event. Track quality requirements are applied, along with momentum and transverse momentum requirements, to reduce combinatorial background. Particle identification criteria are applied to the final-state tracks to suppress background from misidentified particles. To remove cross feed from other charm hadrons, Ξ_c^+ candidates are rejected if they are consistent with $D^+ \to K^+K^-\pi^+$, $D_s^+ \to K^+K^-\pi^+$, $D^+ \to \pi^+K^-\pi^+$, or $D^{*+} \to D^0(K^+K^-)\pi^+$ decays. To reduce background formed from tracks originating at the PV, the decay vertices of Ξ_c^+ and Ξ_b^0 candidates are required to be significantly displaced from all PVs.

The Ξ_c^+ candidates are required to have an invariant mass within $20\,\mathrm{MeV}/c^2$ of the known mass [3], corresponding to approximately $\pm 3\sigma_{\Xi_c^+}$ where $\sigma_{\Xi_c^+}$ is the mass resolution. Candidate Ξ_b^0 decays are required to satisfy $5765 < m_{\mathrm{cand}}(\Xi_b^0) - m_{\mathrm{cand}}(\Xi_c^+) + m_{\Xi_c^+} < 5825\,\mathrm{MeV}/c^2$, where m_{cand} and $m_{\Xi_c^+}$ refer to the candidate and world-average masses, corresponding to approximately $\pm 2\sigma_{\Xi_b^0}$. In addition, the following kinematic requirements are imposed: $p_{\mathrm{T}}(\Xi_c^+) > 1\,\mathrm{GeV}/c$, $p_{\mathrm{T}}(\Xi_b^0) > 2\,\mathrm{GeV}/c$, $p_{\mathrm{T}}(\Xi_b^0\pi_{\mathrm{s}}^-) > 2.5\,\mathrm{GeV}/c$, and $p_{\mathrm{T}}(\pi_{\mathrm{s}}^-) > 0.15\,\mathrm{GeV}/c$. Defining $\delta m \equiv m_{\mathrm{cand}}(\Xi_b^0\pi_{\mathrm{s}}^-) - m_{\mathrm{cand}}(\Xi_b^0) - m_{\pi^-}$, the region of consideration is $\delta m < 45\,\mathrm{MeV}/c^2$. There are on average 1.15 candidates retained in this region per event. Such multiple candidates are due almost entirely to cases where the same Ξ_b^0 candidate is combined with different π_{s}^- candidates from the same PV. All $\Xi_b^0\pi_s^-$ candidates are kept.

The $m_{\mathrm{cand}}(\Xi_b^0)$ projection of the $\Xi_b^0\pi_{\mathrm{s}}^-$ candidates passing the full selection apart from the $m_{\mathrm{cand}}(\Xi_b^0)$ requirement, but including the δm requirement, is shown in Fig. 1. Control samples, notably wrong-sign combinations $\Xi_b^0\pi^+$, are also used to study backgrounds. The δm spectra for the signal and the wrong-sign sample are shown in Fig. 2. Two peaks are clearly visible, a narrow one at $\delta m \approx 3.7\,\mathrm{MeV}/c^2$ and a broader one at $\delta m \approx 24\,\mathrm{MeV}/c^2$. No structure is observed in the wrong-sign sample, nor in studies of the Ξ_b^0 mass sidebands.

Accurate determination of the masses, widths, and signal yields of these two states requires knowledge of the signal shapes, and in particular, the mass resolution of the two peaks. These are obtained from simulated decays with δm values of $3.69\,\mathrm{MeV}/c^2$ and $23.69\,\mathrm{MeV}/c^2$, corresponding to the two peaks. The natural widths, Γ, are set to negligible
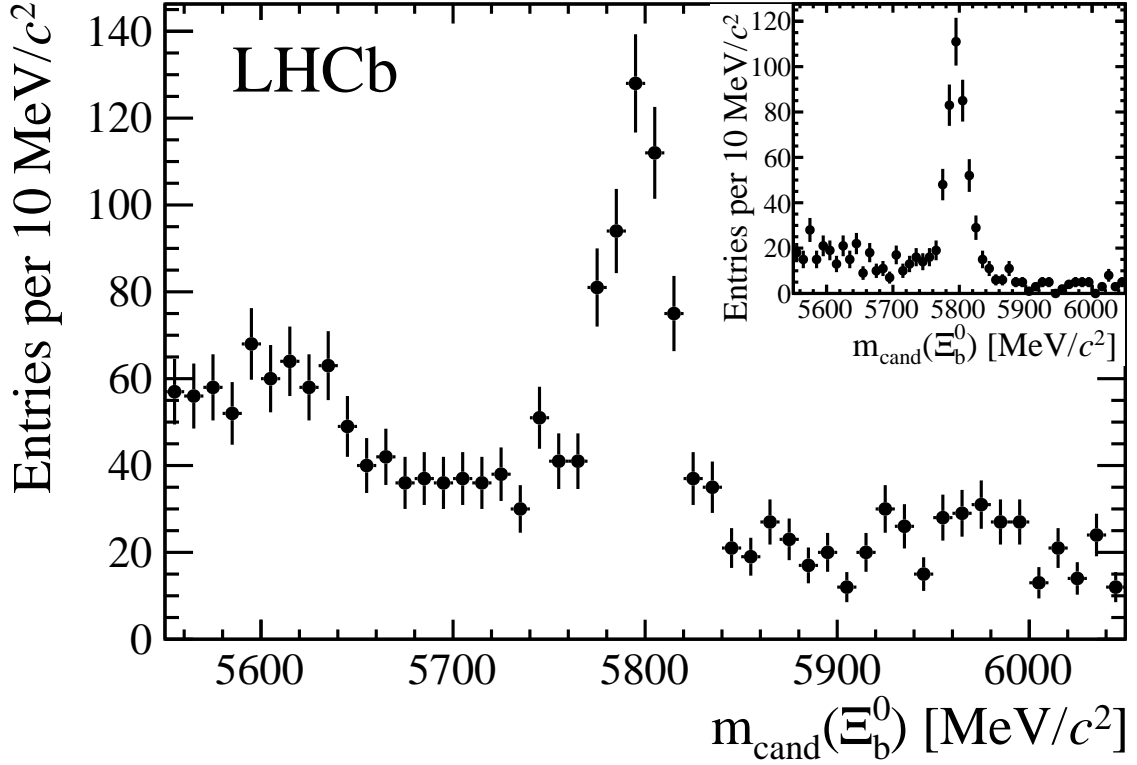
Figure 1: Distribution of $m_{cand}(\Xi_b^0)$ for $\Xi_b^0\pi_s^-$ candidates passing the full selection apart from the $m_{cand}(\Xi_b^0)$ requirement. Inset: The subset of candidates that lie in the δm signal regions of $3.0 < \delta m < 4.2\,\mathrm{MeV}/c^2$ and $21 < \delta m < 27\,\mathrm{MeV}/c^2$.

values so that the width measured in simulation is due entirely to the mass resolution. The resolution function is parameterized as the sum of three Gaussian distributions with independent mean values. Separate sets of parameters are determined for the two peaks. The weighted averages of the three Gaussian widths are $0.21\,\mathrm{MeV}/c^2$ and $0.54\,\mathrm{MeV}/c^2$ for the lower- and higher-mass peaks. In the nominal fits to data, all of the resolution shape parameters are fixed to the values obtained from simulation. Small corrections, obtained from simulation, are applied to the masses to account for offsets in the resolution functions. The combinatorial background is modeled by a threshold function of the form

$$f(\delta m) = \left(1 - e^{-\delta m/C}\right)(\delta m)^A,$$

where A and C are freely varying parameters determined in the fit to the data.

The masses, widths and yields of the two peaks are determined from an unbinned maximum likelihood fit to the δm spectrum. In an initial fit, each peak is described using a P-wave relativistic Breit-Wigner (RBW) line shape [33] with a Blatt-Weisskopf barrier factor [34], convolved with the resolution function obtained from simulation. The fitted width of the lower-mass peak is found to be consistent with zero and consequently its
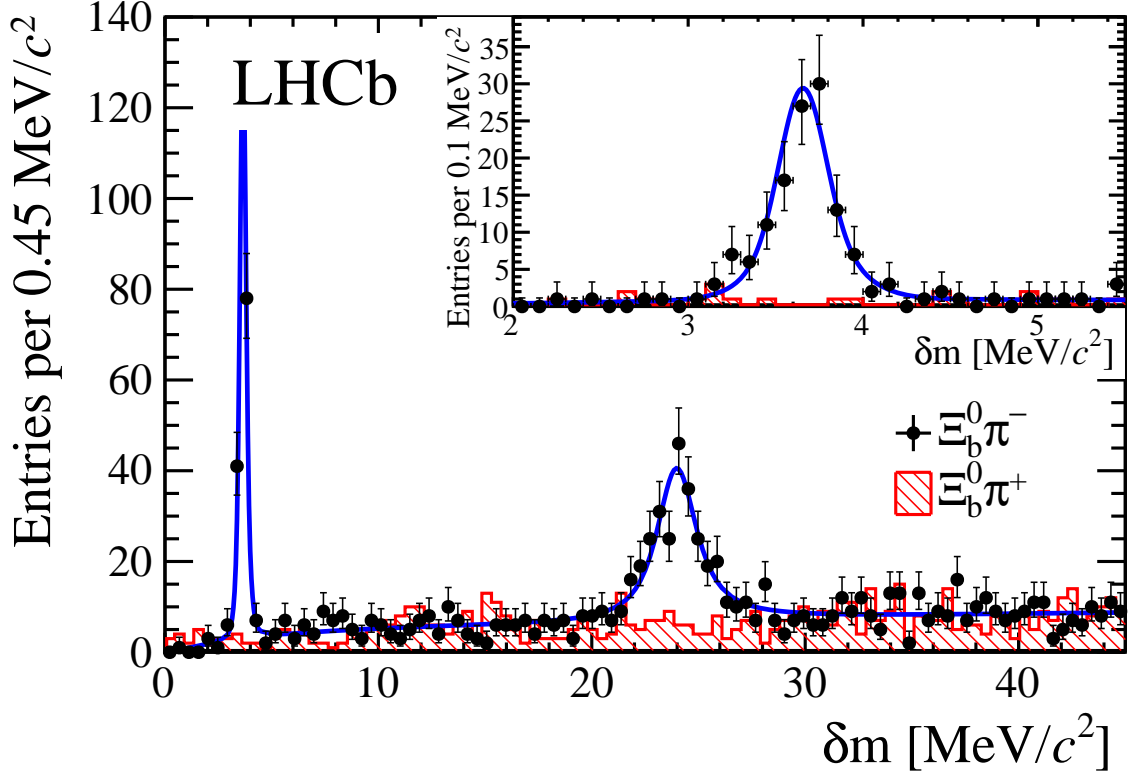
Figure 2: Distribution of the mass difference, δm, for $\Xi_b^0 \pi_s^-$ candidates in data. The points with error bars show right-sign candidates in the Ξ_b^0 mass signal region, and the hatched histogram shows wrong-sign candidates with the same selection. The curve shows the nominal fit to the right-sign candidates. Inset: detail of the region 2.0–5.5 MeV/c^2.

width is set to zero in the nominal fit, shown in Fig. 2. The fitted yields in the lower- and higher-mass peaks are 121 ± 12 and 237 ± 24 events, with statistical significances in excess of 10σ. The nonzero value of the natural width of the higher-mass peak is also highly significant: the change in likelihood when the width is fixed to zero corresponds to a p-value of 4×10^{-14} using Wilks' theorem [35].

An upper limit on the natural width of the lower-mass peak is set using ensembles of pseudoexperiments with the same parameters as in data, but with natural widths ranging from 0.01 to 0.12 MeV. The upper limit is taken to be the value of Γ for which a width equal to or greater than that obtained in data is observed in 95% of the pseudoexperiments. The resulting upper limit is $\Gamma(\Xi_b^{\prime -}) < 0.08$ MeV at 95% confidence level (CL).

A number of cross checks are performed to ensure the robustness of the result and assess systematic uncertainties. These include changing the assumed angular momentum (spin 0, 2) and radial parameter (1–5 GeV $^{-1}$) of the RBW and barrier factor; inflating the widths of the resolution functions by a fixed factor of 1.1, the value found in a large $D^{*+} \to D^0 \pi$ data sample; inflating the widths of the resolution functions by a common factor floated

Table 1: Systematic uncertainties, in units of MeV/c^2 (masses) and MeV (width). The statistical uncertainties are also shown for comparison.

Source	$\delta m(\Xi_b')$	$\delta m(\Xi_b^*)$	$\Gamma(\Xi_b^*)$
Simulated sample size	0.002	0.005	
Multiple candidates	0.004	0.048	0.055
Resolution model	0.002	0.003	0.070
Background description	0.001	0.003	0.019
Momentum scale	0.003	0.014	0.003
RBW spin and radial parameter	0.000	0.023	0.028
Sum in quadrature	0.006	0.055	0.095
Statistical uncertainty	0.018	0.119	0.311

in the fit (with 1.03 ± 0.11 obtained); using a symmetric resolution function; using a non-relativistic BW for the higher-mass peak; using a different background function; varying the fit range; checking the effect of mass dependence of the resolution and finite sample size; keeping only one candidate in each event; imposing additional trigger requirements; separating the data by charge and LHCb magnet polarity; and fitting the wrong-sign sample. Where appropriate, systematic uncertainties are assigned based on the differences between the nominal results and those obtained in these tests. The calibration of the momentum scale is validated by measuring $m(D^{*+}) - m(D^0)$ in a large sample of D^{*+}, $D^0 \to K^-\pi^+$ decays. The mass difference agrees with a recent BaBar measurement [36] within $6\,\mathrm{keV}/c^2$, corresponding to 1.3σ when including the mass scale uncertainty for that decay. The uncertainties are summarized in Table 1. Taking these into account, we obtain

$$
\begin{aligned}
\delta m(\Xi_b'^-) &= 3.653 \pm 0.018 \pm 0.006 \,\mathrm{MeV}/c^2, \\
\delta m(\Xi_b^{*-}) &= 23.96 \pm 0.12 \pm 0.06 \,\mathrm{MeV}/c^2, \\
\Gamma(\Xi_b^{*-}) &= 1.65 \pm 0.31 \pm 0.10 \,\mathrm{MeV}, \\
\Gamma(\Xi_b'^-) &< 0.08 \,\mathrm{MeV} \text{ at } 95\% \text{ CL}.
\end{aligned}
$$

Combining these with the measurement of $m(\Xi_b^0) = 5791.80 \pm 0.50\,\mathrm{MeV}/c^2$ obtained previously at LHCb [9], the masses of these states are found to be

$$
\begin{aligned}
m(\Xi_b'^-) &= 5935.02 \pm 0.02 \pm 0.01 \pm 0.50 \,\mathrm{MeV}/c^2, \\
m(\Xi_b^{*-}) &= 5955.33 \pm 0.12 \pm 0.06 \pm 0.50 \,\mathrm{MeV}/c^2,
\end{aligned}
$$

where the uncertainties are statistical, systematic, and due to the $m(\Xi_b^0)$ measurement, respectively.

Helicity angle [37] distributions may be used to distinguish between spin hypotheses for resonances. We consider the decay sequence $\Xi_b^{(\prime,*)-} \to \Xi_b^0\pi^-$, $\Xi_b^0 \to \Xi_c^+\pi^-$, where the $\Xi_b^{(\prime,*)-}$ has spin J and the Ξ_b^0, Ξ_c^+, and π^- have spin-parity $\frac{1}{2}^+$, $\frac{1}{2}^+$, and 0^-, respectively,

which is analogous to the scenario considered in Ref. [38]. Defining θ_h as the angle between the three-momentum of the Ξ_b^0 in the $\Xi_b^{(\prime,*)-}$ rest frame and the three-momentum of the Ξ_c^+ in the Ξ_b^0 rest frame, the $\cos\theta_h$ distribution is a polynomial of order $(2J-1)$. For $J = \frac{1}{2}$ this would yield a flat distribution, and hence a nonuniform distribution would imply $J > \frac{1}{2}$. The converse does not follow, however: a higher-spin resonance that is unpolarized will lead to a flat distribution. For each of the two peaks, the background-subtracted, efficiency-corrected $\cos\theta_h$ distributions are studied. Both are found to be consistent with flat distributions. When fitted with a function of the form $f(\cos\theta_h) = \left[a + 3(1-a)\cos^2\theta_h\right]/2$, the fitted values of a are 0.89 ± 0.11 and 0.88 ± 0.11, and the quality of the fits does not improve significantly. Thus, the available data are consistent with the quark model expectations that the lower-mass peak corresponds to a $J = \frac{1}{2}$ state and the higher one to a $J = \frac{3}{2}$ state (if unpolarized or weakly polarized), but other values of J are not excluded.

We measure the production rates of the two signals relative to that of the Ξ_b^0 state, selected inclusively and passing the same Ξ_b^0 selection criteria as the signal sample. A downscaling factor of 0.1 was applied in the preselection of the normalization sample for rate reduction purposes. To ensure that the efficiencies are well understood, we use only the subset of events in which one or more of the Ξ_b^0 decay products is consistent with activating the hardware trigger in the calorimeter.

For this subsample of events, the fitted yields are 93 ± 10 for the lower-mass $\Xi_b^0\pi_s^-$ state, 166 ± 20 for the higher-mass $\Xi_b^0\pi_s^-$ state, and 162 ± 15 for the downscaled Ξ_b^0 normalization sample. The efficiency ratios are determined with simulated decays, applying the same trigger, reconstruction, and selection procedures that are used for the data. Systematic uncertainties on these ratios (and, where appropriate, corrections) are assigned for the modeling of the Ξ_b momentum spectra, the π_s^- reconstruction efficiency, the fit method, and the efficiency of those selection criteria that are applied to the $\Xi_b^0\pi_s^-$ candidates but not to the Ξ_b^0 normalization mode. Combining the 7 TeV and 8 TeV data samples, the results obtained are

$$\frac{\sigma(pp \to \Xi_b^{\prime-}X)\mathcal{B}(\Xi_b^{\prime-} \to \Xi_b^0\pi^-)}{\sigma(pp \to \Xi_b^0 X)} = 0.118 \pm 0.017 \pm 0.007,$$

$$\frac{\sigma(pp \to \Xi_b^{*-}X)\mathcal{B}(\Xi_b^{*-} \to \Xi_b^0\pi^-)}{\sigma(pp \to \Xi_b^0 X)} = 0.207 \pm 0.032 \pm 0.015,$$

$$\frac{\sigma(pp \to \Xi_b^{*-}X)\mathcal{B}(\Xi_b^{*-} \to \Xi_b^0\pi^-)}{\sigma(pp \to \Xi_b^{\prime-}X)\mathcal{B}(\Xi_b^{\prime-} \to \Xi_b^0\pi^-)} = 1.74 \pm 0.30 \pm 0.12,$$

where the first and second uncertainties are statistical and systematic, respectively, σ denotes a cross-section measured within the LHCb acceptance and extrapolated to the full kinematic range with PYTHIA, $\mathcal{B}$ represents a branching fraction, and X refers to the rest of the event. Given that isospin partner modes $\Xi_b^{\prime0} \to \Xi_b^0\pi^0$ and $\Xi_b^{*0} \to \Xi_b^0\pi^0$ are also expected, these results imply that a large fraction of Ξ_b^0 baryons in the forward region are produced in the decays of Ξ_b resonances.

As a further check, the $\Xi_b^0\pi_s^-$ mass spectrum is studied with additional Ξ_b^0 decay modes. Significant peaks are seen with the mode $\Xi_b^0 \to \Lambda_c^+(pK^-\pi^+)K^-\pi^+\pi^-$ for both

$\Xi_b'^-$ (6.4σ) and Ξ_b^{*-} (4.7σ). The peaks are also seen with reduced significance in other Ξ_b^0 final states: 4σ for $\Xi_b'^-$ and 2σ for Ξ_b^{*-} in $\Xi_b^0 \to D^0(K^-\pi^+)pK^-$; and 3$\sigma$ for $\Xi_b'^-$ and 3σ for Ξ_b^{*-} in $\Xi_b^0 \to D^+(K^-\pi^+\pi^+)pK^-\pi^-$. The modes $\Xi_b^0 \to \Lambda_c^+(pK^-\pi^+)K^-\pi^+\pi^-$ and $\Xi_b^0 \to D^+(K^-\pi^+\pi^+)pK^-\pi^-$ have not been observed before, and are being studied in separate analyses.

With a specific configuration of other excited Ξ_b states, it is possible to produce a narrow peak in the $\Xi_b^0\pi^-$ mass spectrum that is not due to a $\Xi_b'^-$ resonance. This can arise from the decay chain $\Xi_b^{**-} \to \Xi_b'^0\pi^-$, $\Xi_b'^0 \to \Xi_b^0\pi^0$, where the Ξ_b^{**-} is the $L = 1$, $J^P = \frac{1}{2}^-$ state analagous to the $\Xi_c(2790)$. If both decays are close to threshold, the particles produced will be kinematically correlated such that combining the Ξ_b^0 daughter with the π^- from the Ξ_b^{**-} would produce a structure in the $m(\Xi_b^0\pi^-)$ spectrum. In general such a structure would be broader than that seen in Fig. 2 and would be accompanied by a similar peak in the wrong-sign $\Xi_b^0\pi^+$ spectrum from the isospin-partner decay, $\Xi_b^{**0} \to \Xi_b'^-\pi^+$, $\Xi_b'^- \to \Xi_b^0\pi^-$. However, if a number of conditions are fulfilled, including the Ξ_b^{**-} and $\Xi_b'^0$ states being 279.0 ± 0.5 and 135.8 ± 0.5 MeV/c^2 heavier than the Ξ_b^0 ground state, respectively, it is possible to circumvent these constraints. This would also require that the production rate of the $L = 1$ state be comparable to that of the $L = 0$, $J^P = \frac{3}{2}^+$ state. Although this scenario is contrived, it cannot be excluded at present.

In conclusion, two structures are observed with high significance in the $\Xi_b^0\pi^-$ mass spectrum with mass differences above threshold of $\delta m = 3.653 \pm 0.018 \pm 0.006$ MeV/c^2 and $23.96 \pm 0.12 \pm 0.06$ MeV/c^2. These values are in general agreement with quark model expectations for the $J^P = \frac{1}{2}^+$ $\Xi_b'^-$ and $J^P = \frac{3}{2}^+$ Ξ_b^{*-} states. Their natural widths are measured to be $\Gamma(\Xi_b'^-) < 0.08$ MeV at 95% CL and $\Gamma(\Xi_b^{*-}) = 1.65 \pm 0.31 \pm 0.10$ MeV. The observed angular distributions in the decays of these states are consistent with the spins expected in the quark model, but other other J values are not excluded. The relative production rates are also measured.

References

[1] M. Gell-Mann, *A schematic model of baryons and mesons*, Phys. Lett. **8** (1964) 214.

[2] G. Zweig, *An SU(3) model for strong interaction symmetry and its breaking*, CERN-TH-412, reprinted in Developments in the Quark Theory of Hadrons **1** (2007) 22 (ed. D. Lichtenberg and S. Rosen).

[3] Particle Data Group, K. A. Olive *et al.*, *Review of particle physics*, Chin. Phys. **C38** (2014) 090001.

[4] CDF collaboration, T. Aaltonen *et al.*, *Observation and mass measurement of the baryon* Ξ_b^-, Phys. Rev. Lett. **99** (2007) 052002, `arXiv:0707.0589`.

[5] D0 collaboration, V. Abazov *et al.*, *Direct observation of the strange b baryon* Ξ_b^-, Phys. Rev. Lett. **99** (2007) 052001, `arXiv:0706.1690`.

[6] CDF collaboration, T. Aaltonen *et al.*, *Observation of the* Ω_b^- *baryon and measurement of the properties of the* Ξ_b^- *and* Ω_b^- *baryons*, Phys. Rev. **D80** (2009) 072003, `arXiv:0905.3123`.

[7] CDF collaboration, T. Aaltonen *et al.*, *Observation of the* Ξ_b^0 *baryon*, Phys. Rev. Lett. **107** (2011) 102001, `arXiv:1107.4015`.

[8] LHCb collaboration, R. Aaij *et al.*, *Study of beauty baryon decays to* $D^0 p h^-$ *and* $\Lambda_c^+ h^-$ *final states*, Phys. Rev. **D89** (2014) 032001, `arXiv:1311.4823`.

[9] LHCb collaboration, R. Aaij *et al.*, *Precision measurement of the mass and lifetime of the* Ξ_b^0 *baryon*, Phys. Rev. Lett. **113** (2014) 032001, `arXiv:1405.7223`.

[10] CDF collaboration, T. Aaltonen *et al.*, *Mass and lifetime measurements of bottom and charm baryons in* $p\bar{p}$ *collisions at* $\sqrt{s} = 1.96~TeV$, Phys. Rev. **D89** (2014) 072014, `arXiv:1403.8126`.

[11] LHCb collaboration, R. Aaij *et al.*, *Measurements of the* Λ_b^0, Ξ_b^-, *and* Ω_b^- *baryon masses*, Phys. Rev. Lett. **110** (2013) 182001, `arXiv:1302.1072`.

[12] E. Klempt and J.-M. Richard, *Baryon spectroscopy*, Rev. Mod. Phys. **82** (2010) 1095, `arXiv:0901.2055`.

[13] M. Karliner, B. Keren-Zur, H. J. Lipkin, and J. L. Rosner, *The quark model and b baryons*, Annals Phys. **324** (2009) 2, `arXiv:0804.1575`.

[14] R. Lewis and R. Woloshyn, *Bottom baryons from a dynamical lattice QCD simulation*, Phys. Rev. **D79** (2009) 014502, `arXiv:0806.4783`.

[15] D. Ebert, R. Faustov, and V. Galkin, *Masses of heavy baryons in the relativistic quark model*, Phys. Rev. **D72** (2005) 034026, `arXiv:hep-ph/0504112`.

[16] X. Liu *et al.*, *Bottom baryons*, Phys. Rev. **D77** (2008) 014031, `arXiv:0710.0123`.

[17] E. E. Jenkins, *Model-independent bottom baryon mass predictions in the $1/N_c$ expansion*, Phys. Rev. **D77** (2008) 034012, `arXiv:0712.0406`.

[18] M. Karliner, *Heavy quark spectroscopy and prediction of bottom baryon masses*, Nucl. Phys. Proc. Suppl. **187** (2009) 21, `arXiv:0806.4951`.

[19] J.-R. Zhang and M.-Q. Huang, *Heavy baryon spectroscopy in QCD*, Phys. Rev. **D78** (2008) 094015, `arXiv:0811.3266`.

[20] LHCb collaboration, R. Aaij *et al.*, *Precision luminosity measurements at LHCb*, `arXiv:1410.0149`, submitted to JINST.

[21] CMS collaboration, S. Chatrchyan *et al.*, *Observation of a new Ξ_b baryon*, Phys. Rev. Lett. **108** (2012) 252002, `arXiv:1204.5955`.

[22] LHCb collaboration, A. A. Alves Jr. *et al.*, *The LHCb detector at the LHC*, JINST **3** (2008) S08005.

[23] M. Adinolfi *et al.*, *Performance of the LHCb RICH detector at the LHC*, Eur. Phys. J. **C73** (2013) 2431, `arXiv:1211.6759`.

[24] A. A. Alves Jr. *et al.*, *Performance of the LHCb muon system*, JINST **8** (2013) P02022, `arXiv:1211.1346`.

[25] R. Aaij *et al.*, *The LHCb trigger and its performance in 2011*, JINST **8** (2013) P04022, `arXiv:1211.3055`.

[26] V. V. Gligorov and M. Williams, *Efficient, reliable and fast high-level triggering using a bonsai boosted decision tree*, JINST **8** (2013) P02013, `arXiv:1210.6861`.

[27] T. Sjöstrand, S. Mrenna, and P. Skands, *PYTHIA 6.4 physics and manual*, JHEP **05** (2006) 026, `arXiv:hep-ph/0603175`; T. Sjöstrand, S. Mrenna, and P. Skands, *A brief introduction to PYTHIA 8.1*, Comput. Phys. Commun. **178** (2008) 852, `arXiv:0710.3820`.

[28] I. Belyaev *et al.*, *Handling of the generation of primary events in* Gauss, *the LHCb simulation framework*, Nuclear Science Symposium Conference Record (NSS/MIC) **IEEE** (2010) 1155.

[29] D. J. Lange, *The EvtGen particle decay simulation package*, Nucl. Instrum. Meth. **A462** (2001) 152.

[30] P. Golonka and Z. Was, *PHOTOS Monte Carlo: A precision tool for QED corrections in Z and W decays*, Eur. Phys. J. **C45** (2006) 97, `arXiv:hep-ph/0506026`.

[31] Geant4 collaboration, J. Allison *et al.*, *Geant4 developments and applications*, IEEE Trans. Nucl. Sci. **53** (2006) 270; Geant4 collaboration, S. Agostinelli *et al.*, *Geant4: A simulation toolkit*, Nucl. Instrum. Meth. **A506** (2003) 250.

[32] M. Clemencic *et al.*, *The LHCb simulation application*, GAUSS*: Design, evolution and experience*, J. Phys. Conf. Ser. **331** (2011) 032023.

[33] J. D. Jackson, *Remarks on the phenomenological analysis of resonances*, Nuovo Cim. **34** (1964) 1644.

[34] J. Blatt and V. Weisskopf, *Theoretical nuclear physics*, John Wiley & Sons, 1952.

[35] S. Wilks, *The large-sample distribution of the likelihood ratio for testing composite hypotheses*, Annals Math. Statist. **9** (1938) 60.

[36] BaBar collaboration, J. P. Lees *et al.*, *Measurement of the $D^*(2010)^+$ natural line width and the $D^*(2010)^+ - D^0$ mass difference*, Phys. Rev. **D88** (2013) 052003, arXiv:1304.5009; BaBar collaboration, J. P. Lees *et al.*, *Measurement of the $D^*(2010)^+$ meson width and the $D^*(2010)^+ - D^0$ mass difference*, Phys. Rev. Lett. **111** (2013) 111801, arXiv:1304.5657.

[37] J. D. Richman, *An experimenter's guide to the helicity formalism*, CALT-68-1148.

[38] Belle collaboration, K. Abe *et al.*, *Experimental constraints on the spin and parity of the $\Lambda_c(2880)^+$*, Phys. Rev. Lett. **98** (2007) 262001, arXiv:hep-ex/0608043.

LHCb collaboration

R. Aaij[41], B. Adeva[37], M. Adinolfi[46], A. Affolder[52], Z. Ajaltouni[5], S. Akar[6], J. Albrecht[9],
F. Alessio[38], M. Alexander[51], S. Ali[41], G. Alkhazov[30], P. Alvarez Cartelle[37], A.A. Alves Jr[25,38],
S. Amato[2], S. Amerio[22], Y. Amhis[7], L. An[3], L. Anderlini[17,g], J. Anderson[40], R. Andreassen[57],
M. Andreotti[16,f], J.E. Andrews[58], R.B. Appleby[54], O. Aquines Gutierrez[10], F. Archilli[38],
A. Artamonov[35], M. Artuso[59], E. Aslanides[6], G. Auriemma[25,n], M. Baalouch[5], S. Bachmann[11],
J.J. Back[48], A. Badalov[36], C. Baesso[60], W. Baldini[16], R.J. Barlow[54], C. Barschel[38], S. Barsuk[7],
W. Barter[47], V. Batozskaya[28], V. Battista[39], A. Bay[39], L. Beaucourt[4], J. Beddow[51],
F. Bedeschi[23], I. Bediaga[1], S. Belogurov[31], K. Belous[35], I. Belyaev[31], E. Ben-Haim[8],
G. Bencivenni[18], S. Benson[38], J. Benton[46], A. Berezhnoy[32], R. Bernet[40], A. Bertolin[22],
M.-O. Bettler[47], M. van Beuzekom[41], A. Bien[11], S. Bifani[45], T. Bird[54], A. Bizzeti[17,i],
P.M. Bjørnstad[54], T. Blake[48], F. Blanc[39], J. Blouw[10], S. Blusk[59], V. Bocci[25], A. Bondar[34],
N. Bondar[30,38], W. Bonivento[15], S. Borghi[54], A. Borgia[59], M. Borsato[7], T.J.V. Bowcock[52],
E. Bowen[40], C. Bozzi[16], D. Brett[54], M. Britsch[10], T. Britton[59], J. Brodzicka[54], N.H. Brook[46],
A. Bursche[40], J. Buytaert[38], S. Cadeddu[15], R. Calabrese[16,f], M. Calvi[20,k], M. Calvo Gomez[36,p],
P. Campana[18], D. Campora Perez[38], L. Capriotti[54], A. Carbone[14,d], G. Carboni[24,l],
R. Cardinale[19,38,j], A. Cardini[15], L. Carson[50], K. Carvalho Akiba[2,38], RCM Casanova Mohr[36],
G. Casse[52], L. Cassina[20,k], L. Castillo Garcia[38], M. Cattaneo[38], Ch. Cauet[9], R. Cenci[23,t],
M. Charles[8], Ph. Charpentier[38], M. Chefdeville[4], S. Chen[54], S.-F. Cheung[55], N. Chiapolini[40],
M. Chrzaszcz[40,26], X. Cid Vidal[38], G. Ciezarek[41], P.E.L. Clarke[50], M. Clemencic[38], H.V. Cliff[47],
J. Closier[38], V. Coco[38], J. Cogan[6], E. Cogneras[5], V. Cogoni[15], L. Cojocariu[29], G. Collazuol[22],
P. Collins[38], A. Comerma-Montells[11], A. Contu[15,38], A. Cook[46], M. Coombes[46], S. Coquereau[8],
G. Corti[38], M. Corvo[16,f], I. Counts[56], B. Couturier[38], G.A. Cowan[50], D.C. Craik[48],
A.C. Crocombe[48], M. Cruz Torres[60], S. Cunliffe[53], R. Currie[53], C. D'Ambrosio[38], J. Dalseno[46],
P. David[8], P.N.Y. David[41], A. Davis[57], K. De Bruyn[41], S. De Capua[54], M. De Cian[11],
J.M. De Miranda[1], L. De Paula[2], W. De Silva[57], P. De Simone[18], C.-T. Dean[51], D. Decamp[4],
M. Deckenhoff[9], L. Del Buono[8], N. Déléage[4], D. Derkach[55], O. Deschamps[5], F. Dettori[38],
B. Dey[40], A. Di Canto[38], A Di Domenico[25], H. Dijkstra[38], S. Donleavy[52], F. Dordei[11],
M. Dorigo[39], A. Dosil Suárez[37], D. Dossett[48], A. Dovbnya[43], K. Dreimanis[52], G. Dujany[54],
F. Dupertuis[39], P. Durante[38], R. Dzhelyadin[35], A. Dziurda[26], A. Dzyuba[30], S. Easo[49,38],
U. Egede[53], V. Egorychev[31], S. Eidelman[34], S. Eisenhardt[50], U. Eitschberger[9], R. Ekelhof[9],
L. Eklund[51], I. El Rifai[5], Ch. Elsasser[40], S. Ely[59], S. Esen[11], H.-M. Evans[47], T. Evans[55],
A. Falabella[14], C. Färber[11], C. Farinelli[41], N. Farley[45], S. Farry[52], R. Fay[52], D. Ferguson[50],
V. Fernandez Albor[37], F. Ferreira Rodrigues[1], M. Ferro-Luzzi[38], S. Filippov[33], M. Fiore[16,f],
M. Fiorini[16,f], M. Firlej[27], C. Fitzpatrick[39], T. Fiutowski[27], P. Fol[53], M. Fontana[10],
F. Fontanelli[19,j], R. Forty[38], O. Francisco[2], M. Frank[38], C. Frei[38], M. Frosini[17], J. Fu[21,38],
E. Furfaro[24,l], A. Gallas Torreira[37], D. Galli[14,d], S. Gallorini[22,38], S. Gambetta[19,j],
M. Gandelman[2], P. Gandini[59], Y. Gao[3], J. García Pardiñas[37], J. Garofoli[59], J. Garra Tico[47],
L. Garrido[36], D. Gascon[36], C. Gaspar[38], U. Gastaldi[16], R. Gauld[55], L. Gavardi[9], G. Gazzoni[5],
A. Geraci[21,v], E. Gersabeck[11], M. Gersabeck[54], T. Gershon[48], Ph. Ghez[4], A. Gianelle[22],
S. Gianì[39], V. Gibson[47], L. Giubega[29], V.V. Gligorov[38], C. Göbel[60], D. Golubkov[31],
A. Golutvin[53,31,38], A. Gomes[1,a], C. Gotti[20,k], M. Grabalosa Gándara[5], R. Graciani Diaz[36],
L.A. Granado Cardoso[38], E. Graugés[36], E. Graverini[40], G. Graziani[17], A. Grecu[29],
E. Greening[55], S. Gregson[47], P. Griffith[45], L. Grillo[11], O. Grünberg[63], B. Gui[59], E. Gushchin[33],
Yu. Guz[35,38], T. Gys[38], C. Hadjivasiliou[59], G. Haefeli[39], C. Haen[38], S.C. Haines[47], S. Hall[53],

B. Hamilton[58], T. Hampson[46], X. Han[11], S. Hansmann-Menzemer[11], N. Harnew[55],
S.T. Harnew[46], J. Harrison[54], J. He[38], T. Head[39], V. Heijne[41], K. Hennessy[52], P. Henrard[5],
L. Henry[8], J.A. Hernando Morata[37], E. van Herwijnen[38], M. Heß[63], A. Hicheur[2], D. Hill[55],
M. Hoballah[5], C. Hombach[54], W. Hulsbergen[41], N. Hussain[55], D. Hutchcroft[52], D. Hynds[51],
M. Idzik[27], P. Ilten[56], R. Jacobsson[38], A. Jaeger[11], J. Jalocha[55], E. Jans[41], P. Jaton[39],
A. Jawahery[58], F. Jing[3], M. John[55], D. Johnson[38], C.R. Jones[47], C. Joram[38], B. Jost[38],
N. Jurik[59], S. Kandybei[43], W. Kanso[6], M. Karacson[38], T.M. Karbach[38], S. Karodia[51],
M. Kelsey[59], I.R. Kenyon[45], T. Ketel[42], B. Khanji[20,38,k], C. Khurewathanakul[39], S. Klaver[54],
K. Klimaszewski[28], O. Kochebina[7], M. Kolpin[11], I. Komarov[39], R.F. Koopman[42],
P. Koppenburg[41,38], M. Korolev[32], L. Kravchuk[33], K. Kreplin[11], M. Kreps[48], G. Krocker[11],
P. Krokovny[34], F. Kruse[9], W. Kucewicz[26,o], M. Kucharczyk[20,26,k], V. Kudryavtsev[34],
K. Kurek[28], T. Kvaratskheliya[31], V.N. La Thi[39], D. Lacarrere[38], G. Lafferty[54], A. Lai[15],
D. Lambert[50], R.W. Lambert[42], G. Lanfranchi[18], C. Langenbruch[48], B. Langhans[38],
T. Latham[48], C. Lazzeroni[45], R. Le Gac[6], J. van Leerdam[41], J.-P. Lees[4], R. Lefèvre[5],
A. Leflat[32], J. Lefrançois[7], O. Leroy[6], T. Lesiak[26], B. Leverington[11], Y. Li[3], T. Likhomanenko[64],
M. Liles[52], R. Lindner[38], C. Linn[38], F. Lionetto[40], B. Liu[15], S. Lohn[38], I. Longstaff[51],
J.H. Lopes[2], P. Lowdon[40], D. Lucchesi[22,r], H. Luo[50], A. Lupato[22], E. Luppi[16,f], O. Lupton[55],
F. Machefert[7], I.V. Machikhiliyan[31], F. Maciuc[29], O. Maev[30], S. Malde[55], A. Malinin[64],
G. Manca[15,e], G. Mancinelli[6], A. Mapelli[38], J. Maratas[5], J.F. Marchand[4], U. Marconi[14],
C. Marin Benito[36], P. Marino[23,t], R. Märki[39], J. Marks[11], G. Martellotti[25], M. Martinelli[39],
D. Martinez Santos[42], F. Martinez Vidal[65], D. Martins Tostes[2], A. Massafferri[1], R. Matev[38],
Z. Mathe[38], C. Matteuzzi[20], A. Mazurov[45], M. McCann[53], J. McCarthy[45], A. McNab[54],
R. McNulty[12], B. McSkelly[52], B. Meadows[57], F. Meier[9], M. Meissner[11], M. Merk[41],
D.A. Milanes[62], M.-N. Minard[4], N. Moggi[14], J. Molina Rodriguez[60], S. Monteil[5], M. Morandin[22],
P. Morawski[27], A. Mordà[6], M.J. Morello[23,t], J. Moron[27], A.-B. Morris[50], R. Mountain[59],
F. Muheim[50], K. Müller[40], M. Mussini[14], B. Muster[39], P. Naik[46], T. Nakada[39],
R. Nandakumar[49], I. Nasteva[2], M. Needham[50], N. Neri[21], S. Neubert[38], N. Neufeld[38],
M. Neuner[11], A.D. Nguyen[39], T.D. Nguyen[39], C. Nguyen-Mau[39,q], M. Nicol[7], V. Niess[5],
R. Niet[9], N. Nikitin[32], T. Nikodem[11], A. Novoselov[35], D.P. O'Hanlon[48],
A. Oblakowska-Mucha[27], V. Obraztsov[35], S. Ogilvy[51], O. Okhrimenko[44], R. Oldeman[15,e],
C.J.G. Onderwater[66], M. Orlandea[29], J.M. Otalora Goicochea[2], A. Otto[38], P. Owen[53],
A. Oyanguren[65], B.K. Pal[59], A. Palano[13,c], F. Palombo[21,u], M. Palutan[18], J. Panman[38],
A. Papanestis[49,38], M. Pappagallo[51], L.L. Pappalardo[16,f], C. Parkes[54], C.J. Parkinson[9,45],
G. Passaleva[17], G.D. Patel[52], M. Patel[53], C. Patrignani[19,j], A. Pearce[54,49], A. Pellegrino[41],
G. Penso[25,m], M. Pepe Altarelli[38], S. Perazzini[14,d], P. Perret[5], L. Pescatore[45], E. Pesen[67],
K. Petridis[53], A. Petrolini[19,j], E. Picatoste Olloqui[36], B. Pietrzyk[4], T. Pilař[48], D. Pinci[25],
A. Pistone[19], S. Playfer[50], M. Plo Casasus[37], F. Polci[8], A. Poluektov[48,34], I. Polyakov[31],
E. Polycarpo[2], A. Popov[35], D. Popov[10], B. Popovici[29], C. Potterat[2], E. Price[46], J.D. Price[52],
J. Prisciandaro[39], A. Pritchard[52], C. Prouve[46], V. Pugatch[44], A. Puig Navarro[39], G. Punzi[23,s],
W. Qian[4], B. Rachwal[26], J.H. Rademacker[46], B. Rakotomiaramanana[39], M. Rama[23],
M.S. Rangel[2], I. Raniuk[43], N. Rauschmayr[38], G. Raven[42], F. Redi[53], S. Reichert[54], M.M. Reid[48],
A.C. dos Reis[1], S. Ricciardi[49], S. Richards[46], M. Rihl[38], K. Rinnert[52], V. Rives Molina[36],
P. Robbe[7], A.B. Rodrigues[1], E. Rodrigues[54], P. Rodriguez Perez[54], S. Roiser[38],
V. Romanovsky[35], A. Romero Vidal[37], M. Rotondo[22], J. Rouvinet[39], T. Ruf[38], H. Ruiz[36],
P. Ruiz Valls[65], J.J. Saborido Silva[37], N. Sagidova[30], P. Sail[51], B. Saitta[15,e],
V. Salustino Guimaraes[2], C. Sanchez Mayordomo[65], B. Sanmartin Sedes[37], R. Santacesaria[25],

C. Santamarina Rios[37], E. Santovetti[24,l], A. Sarti[18,m], C. Satriano[25,n], A. Satta[24],
D.M. Saunders[46], D. Savrina[31,32], M. Schiller[38], H. Schindler[38], M. Schlupp[9], M. Schmelling[10],
B. Schmidt[38], O. Schneider[39], A. Schopper[38], M.-H. Schune[7], R. Schwemmer[38], B. Sciascia[18],
A. Sciubba[25,m], A. Semennikov[31], I. Sepp[53], N. Serra[40], J. Serrano[6], L. Sestini[22], P. Seyfert[11],
M. Shapkin[35], I. Shapoval[16,43,f], Y. Shcheglov[30], T. Shears[52], L. Shekhtman[34], V. Shevchenko[64],
A. Shires[9], R. Silva Coutinho[48], G. Simi[22], M. Sirendi[47], N. Skidmore[46], I. Skillicorn[51],
T. Skwarnicki[59], N.A. Smith[52], E. Smith[55,49], E. Smith[53], J. Smith[47], M. Smith[54], H. Snoek[41],
M.D. Sokoloff[57], F.J.P. Soler[51], F. Soomro[39], D. Souza[46], B. Souza De Paula[2], B. Spaan[9],
P. Spradlin[51], S. Sridharan[38], F. Stagni[38], M. Stahl[11], S. Stahl[11], O. Steinkamp[40],
O. Stenyakin[35], F Sterpka[59], S. Stevenson[55], S. Stoica[29], S. Stone[59], B. Storaci[40], S. Stracka[23,t],
M. Straticiuc[29], U. Straumann[40], R. Stroili[22], L. Sun[57], W. Sutcliffe[53], K. Swientek[27],
S. Swientek[9], V. Syropoulos[42], M. Szczekowski[28], P. Szczypka[39,38], T. Szumlak[27],
S. T'Jampens[4], M. Teklishyn[7], G. Tellarini[16,f], F. Teubert[38], C. Thomas[55], E. Thomas[38],
J. van Tilburg[41], V. Tisserand[4], M. Tobin[39], J. Todd[57], S. Tolk[42], L. Tomassetti[16,f],
D. Tonelli[38], S. Topp-Joergensen[55], N. Torr[55], E. Tournefier[4], S. Tourneur[39], M.T. Tran[39],
M. Tresch[40], A. Trisovic[38], A. Tsaregorodtsev[6], P. Tsopelas[41], N. Tuning[41], M. Ubeda Garcia[38],
A. Ukleja[28], A. Ustyuzhanin[64], U. Uwer[11], C. Vacca[15], V. Vagnoni[14], G. Valenti[14], A. Vallier[7],
R. Vazquez Gomez[18], P. Vazquez Regueiro[37], C. Vázquez Sierra[37], S. Vecchi[16], J.J. Velthuis[46],
M. Veltri[17,h], G. Veneziano[39], M. Vesterinen[11], JVVB Viana Barbosa[38], B. Viaud[7], D. Vieira[2],
M. Vieites Diaz[37], X. Vilasis-Cardona[36,p], A. Vollhardt[40], D. Volyanskyy[10], D. Voong[46],
A. Vorobyev[30], V. Vorobyev[34], C. Voß[63], J.A. de Vries[41], R. Waldi[63], C. Wallace[48], R. Wallace[12],
J. Walsh[23], S. Wandernoth[11], J. Wang[59], D.R. Ward[47], N.K. Watson[45], D. Websdale[53],
M. Whitehead[48], D. Wiedner[11], G. Wilkinson[55,38], M. Wilkinson[59], M.P. Williams[45],
M. Williams[56], H.W. Wilschut[66], F.F. Wilson[49], J. Wimberley[58], J. Wishahi[9], W. Wislicki[28],
M. Witek[26], G. Wormser[7], S.A. Wotton[47], S. Wright[47], K. Wyllie[38], Y. Xie[61], Z. Xing[59],
Z. Xu[39], Z. Yang[3], X. Yuan[3], O. Yushchenko[35], M. Zangoli[14], M. Zavertyaev[10,b], L. Zhang[3],
W.C. Zhang[12], Y. Zhang[3], A. Zhelezov[11], A. Zhokhov[31], L. Zhong[3].

[1] Centro Brasileiro de Pesquisas Físicas (CBPF), Rio de Janeiro, Brazil
[2] Universidade Federal do Rio de Janeiro (UFRJ), Rio de Janeiro, Brazil
[3] Center for High Energy Physics, Tsinghua University, Beijing, China
[4] LAPP, Université de Savoie, CNRS/IN2P3, Annecy-Le-Vieux, France
[5] Clermont Université, Université Blaise Pascal, CNRS/IN2P3, LPC, Clermont-Ferrand, France
[6] CPPM, Aix-Marseille Université, CNRS/IN2P3, Marseille, France
[7] LAL, Université Paris-Sud, CNRS/IN2P3, Orsay, France
[8] LPNHE, Université Pierre et Marie Curie, Université Paris Diderot, CNRS/IN2P3, Paris, France
[9] Fakultät Physik, Technische Universität Dortmund, Dortmund, Germany
[10] Max-Planck-Institut für Kernphysik (MPIK), Heidelberg, Germany
[11] Physikalisches Institut, Ruprecht-Karls-Universität Heidelberg, Heidelberg, Germany
[12] School of Physics, University College Dublin, Dublin, Ireland
[13] Sezione INFN di Bari, Bari, Italy
[14] Sezione INFN di Bologna, Bologna, Italy
[15] Sezione INFN di Cagliari, Cagliari, Italy
[16] Sezione INFN di Ferrara, Ferrara, Italy
[17] Sezione INFN di Firenze, Firenze, Italy
[18] Laboratori Nazionali dell'INFN di Frascati, Frascati, Italy
[19] Sezione INFN di Genova, Genova, Italy
[20] Sezione INFN di Milano Bicocca, Milano, Italy
[21] Sezione INFN di Milano, Milano, Italy

[22]*Sezione INFN di Padova, Padova, Italy*

[23]*Sezione INFN di Pisa, Pisa, Italy*

[24]*Sezione INFN di Roma Tor Vergata, Roma, Italy*

[25]*Sezione INFN di Roma La Sapienza, Roma, Italy*

[26]*Henryk Niewodniczanski Institute of Nuclear Physics Polish Academy of Sciences, Kraków, Poland*

[27]*AGH - University of Science and Technology, Faculty of Physics and Applied Computer Science, Kraków, Poland*

[28]*National Center for Nuclear Research (NCBJ), Warsaw, Poland*

[29]*Horia Hulubei National Institute of Physics and Nuclear Engineering, Bucharest-Magurele, Romania*

[30]*Petersburg Nuclear Physics Institute (PNPI), Gatchina, Russia*

[31]*Institute of Theoretical and Experimental Physics (ITEP), Moscow, Russia*

[32]*Institute of Nuclear Physics, Moscow State University (SINP MSU), Moscow, Russia*

[33]*Institute for Nuclear Research of the Russian Academy of Sciences (INR RAN), Moscow, Russia*

[34]*Budker Institute of Nuclear Physics (SB RAS) and Novosibirsk State University, Novosibirsk, Russia*

[35]*Institute for High Energy Physics (IHEP), Protvino, Russia*

[36]*Universitat de Barcelona, Barcelona, Spain*

[37]*Universidad de Santiago de Compostela, Santiago de Compostela, Spain*

[38]*European Organization for Nuclear Research (CERN), Geneva, Switzerland*

[39]*Ecole Polytechnique Fédérale de Lausanne (EPFL), Lausanne, Switzerland*

[40]*Physik-Institut, Universität Zürich, Zürich, Switzerland*

[41]*Nikhef National Institute for Subatomic Physics, Amsterdam, The Netherlands*

[42]*Nikhef National Institute for Subatomic Physics and VU University Amsterdam, Amsterdam, The Netherlands*

[43]*NSC Kharkiv Institute of Physics and Technology (NSC KIPT), Kharkiv, Ukraine*

[44]*Institute for Nuclear Research of the National Academy of Sciences (KINR), Kyiv, Ukraine*

[45]*University of Birmingham, Birmingham, United Kingdom*

[46]*H.H. Wills Physics Laboratory, University of Bristol, Bristol, United Kingdom*

[47]*Cavendish Laboratory, University of Cambridge, Cambridge, United Kingdom*

[48]*Department of Physics, University of Warwick, Coventry, United Kingdom*

[49]*STFC Rutherford Appleton Laboratory, Didcot, United Kingdom*

[50]*School of Physics and Astronomy, University of Edinburgh, Edinburgh, United Kingdom*

[51]*School of Physics and Astronomy, University of Glasgow, Glasgow, United Kingdom*

[52]*Oliver Lodge Laboratory, University of Liverpool, Liverpool, United Kingdom*

[53]*Imperial College London, London, United Kingdom*

[54]*School of Physics and Astronomy, University of Manchester, Manchester, United Kingdom*

[55]*Department of Physics, University of Oxford, Oxford, United Kingdom*

[56]*Massachusetts Institute of Technology, Cambridge, MA, United States*

[57]*University of Cincinnati, Cincinnati, OH, United States*

[58]*University of Maryland, College Park, MD, United States*

[59]*Syracuse University, Syracuse, NY, United States*

[60]*Pontifícia Universidade Católica do Rio de Janeiro (PUC-Rio), Rio de Janeiro, Brazil, associated to* [2]

[61]*Institute of Particle Physics, Central China Normal University, Wuhan, Hubei, China, associated to* [3]

[62]*Departamento de Fisica , Universidad Nacional de Colombia, Bogota, Colombia, associated to* [8]

[63]*Institut für Physik, Universität Rostock, Rostock, Germany, associated to* [11]

[64]*National Research Centre Kurchatov Institute, Moscow, Russia, associated to* [31]

[65]*Instituto de Fisica Corpuscular (IFIC), Universitat de Valencia-CSIC, Valencia, Spain, associated to* [36]

[66]*Van Swinderen Institute, University of Groningen, Groningen, The Netherlands, associated to* [41]

[67]*Celal Bayar University, Manisa, Turkey, associated to* [38]

[a]*Universidade Federal do Triângulo Mineiro (UFTM), Uberaba-MG, Brazil*

[b]*P.N. Lebedev Physical Institute, Russian Academy of Science (LPI RAS), Moscow, Russia*

[c]*Università di Bari, Bari, Italy*

[d]*Università di Bologna, Bologna, Italy*

[e]*Università di Cagliari, Cagliari, Italy*

[f]*Università di Ferrara, Ferrara, Italy*

[g]*Università di Firenze, Firenze, Italy*

[h]*Università di Urbino, Urbino, Italy*

[i]*Università di Modena e Reggio Emilia, Modena, Italy*

[j]*Università di Genova, Genova, Italy*

[k]*Università di Milano Bicocca, Milano, Italy*

[l]*Università di Roma Tor Vergata, Roma, Italy*

[m]*Università di Roma La Sapienza, Roma, Italy*

[n]*Università della Basilicata, Potenza, Italy*

[o]*AGH - University of Science and Technology, Faculty of Computer Science, Electronics and Telecommunications, Kraków, Poland*

[p]*LIFAELS, La Salle, Universitat Ramon Llull, Barcelona, Spain*

[q]*Hanoi University of Science, Hanoi, Viet Nam*

[r]*Università di Padova, Padova, Italy*

[s]*Università di Pisa, Pisa, Italy*

[t]*Scuola Normale Superiore, Pisa, Italy*

[u]*Università degli Studi di Milano, Milano, Italy*

[v]*Politecnico di Milano, Milano, Italy*